Received: 27 March 2023 | *Revised:* 7 May 2023 | *Accepted:* 19 May 2023
DOI: 10.37917/ijeee.19.2.15 *Vol. 19 | Issue 2 | December 2023*

Iraqi Journal for Electrical and Electronic Engineering
Original Article

Open Access
IJEEE University of Basrah College of Engineering

Separate and Combined Effective Coding of Bit Planes of Grayscale Images

Oday Jasim Mohammed Al-Furaiji*[1], Viktar Yurevich Tsviatkou[2], Baqir Jafar Sadiq[2]
[1]Computer Science Department, Shatt Al-Arab University College, Basra, Iraq
[2]Department of Infocommunication Technologies, Belarusian State University of Informatics and Radioelectronics, Minsk, Belarus

Correspondance
*Oday Jasim Mohammed Al-Furaiji
Department of Computer Science,
Shatt Al-Arab University College, Basra, Iraq.
Email: odaymohammed@mail.ru

Abstract
Currently, an approach involving a coder with a combined structure for compressing images combining several different coders, the system for connecting them to various bit planes, and the control system for these connections have not been studied. Thus, there is a need to develop a structure and study the effectiveness of a combined codec for compressing images of various types without loss in the spatial domain based on arithmetic and (Run-Length Encoding) RLE-coding algorithms. The essence of separate effective coding is to use independent coders of the same type or one coder connected to the planes alternately in order to compress the higher and lower bit planes of the image or their combinations. In this paper, the results of studying the effectiveness of using a combination of arithmetic and RLE coding for several types of images are presented. As a result of developing this structure, the effectiveness of combined coding for compressing the differences in the channels of hyperspectral images (HSI) has been established, as hyperspectral images consist of multi-spectral bands, instead of just the typical three bands (RGB) or (YCbCr) found in regular images. Where, each pixel in a hyperspectral image represents the entire spectrum of light reflected by the object or scene at that particular location.

Keywords
Combined effective coding, Lossless image compression, Arithmetic coding, RLE coding, Bit planes, Hyperspectral images.

I. Introduction

On images of various types, the highest compression ratio is shown by different codecs. This is due to the fact, that the distributions of values in the bit-planes of images are different [1–6]. It can also be assumed that different bit-planes of one image can be better compressed using different codecs. Thus, for images of various types (satellite, medical, thermal, hyperspectral, etc.), the highest compression ratios are possible with various combinations of codecs of bit-planes.This approach involves a coder for image compression with a combined structure that combines several different coders, and the system for connecting them to different bit planes and also the system for managing these connections, is not practically explored at present. In the modern image compression codecs [7–16], one processing algorithm for all bit planes is used. Indirect confirmations of the efficiency of combined coding can be found in EZW, SPIHT, SPECK codec structures [17–19], which provide separate coding of bit planes and provide the possibility of using the lower bit planes with equiprobable repetition of zeros and ones without coding, as well as in the JPEG 2000 codec structure [11], which provides the possibility of using two algorithms for image compression lossless and lossy. However, in the considered codecs, different coding algorithms are not applied to different bit

planes. The efficiency of separate coding of bit planes is analyzed in [20, 21], but only for the RLE coder [22]. The results of studying the effectiveness of using a combination of arithmetic and RLE-coding are presented in [21], but only for several types of images. Insufficient study of the combined approach to image coding is associated with an increase in computational complexity: time (due to the additional cost of choosing the encoding algorithm) and spatial (due to the additional memory cost for implementing several encoding algorithms).However, with the development of the element base, the increase in the computational complexity of coding becomes less critical compared to an increase in the compression ratio, especially for applications involving the transmission of images in real time through channels with limited bandwidth. In addition, it is possible to use a combination of codecs with a complex and simple structure, which leads to a relatively small increase in computational complexity. The most interesting in this regard are arithmetic [23] and RLE [22] codecs. The arithmetic codec is a part of the JPEG 2000 codec core and allows to achieve high image compression ratios. The RLE-codec has a relatively low computational complexity, because it has found a widespread use as a part of various image compression codecs and archivers.

The aim of this work is to develop the structure and study the effectiveness of a combined codec for compressing images of various types without loss in the spatial domain, based on arithmetic and RLE coding algorithms.

II. Separate Effective Coding of Bit Planes of Images

To develop the structure of a combined image compression lossless codec in the spatial domain, a study of the effectiveness of separate coding of bit-plane images using arithmetic and RLE coders was conducted. The essence of separate effective coding is to use for compression the high and low image bit planes or their combinations of independent coders of the same type or one coder connected to the planes alternately, as shown in Fig. 1.

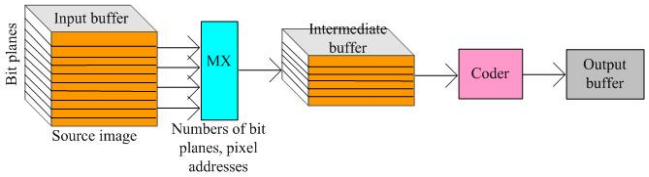

Fig. 1. Separate effective coding of image bit planes scheme

Bit planes $B(r)$ are formed from the same bits of r pixels $i(R,y,x)$ of an R-bit image $I(R) = \|i(R,y,x))\|_{(y=0,\overline{Y-1},x=0,\overline{X-1})}$ and represent a matrix $B(r) = \|b(r,y,x))\|_{(y=0,\overline{Y-1},x=0,\overline{X-1})}$, consisting of zeros and ones $(b(r,y,x) = \{0,1\})$, the size $Y \times X$ of which coincides with the size $Y \times X$ of the original image $I(R)$. The values $i(R,y,x)$ and $b(r,y,x)$ are related by (1).

$$i(R,y,x) = \sum_{r=0}^{R-1} 2^r b(r,y,x) \tag{1}$$

at $y = \overline{0,Y-1}$, $x = \overline{0,X-1}$.

The combination of multiple r_C bit planes $(0 < r_C < R)$ from r_L to r_H $(r_H > r_L, r_C = r_H - r_L + 1)$ represents a matrix $I_C(r_L,r_H) = \|i_C(r_L,r_H,y,x)\|_{(y=\overline{0,Y-1},x=\overline{0,X-1})}$, the values $i_C(r_L,r_H,y,x)$ of which have r_C bits, will be expressed by (2).

$$i_C(r_L,r_H,y,x) = \sum_{r=r_L}^{r_H} 2^{r-r_L} b(r,y,x) \tag{2}$$

at $y = \overline{0,Y-1}$, $x = \overline{0,X-1}$.

For a special case $r_H = r_L$, the equality holds $i_C(r_L,r_H,y,x) = b(r_L,y,x)$.

Tables (I, II, and III) show the average compression ratios of the bit planes of 8-bit $(R = 8)$ satellite, portrait, medical grayscale, and landscape thermal images Fig. 2(a), as well as the differences of spectral channels of 16-bit $(R = 16)$ hyperspectral images (HSI), as shown in Fig. 2(b). The RLE and arithmetic coders (AC) are used for compression. The averaging of values of compression coefficients is made on 8 test images of each type.

Fig. 2. Examples of images
(a) 8-bit grayscale image; (b) differences of spectral channels of 16-bit hyperspectral image

The RLE coder is applied separately for each bit plane $(f_{RLE}(B(r))$ at $r = \overline{0,R-1})$, where f_{RLE} – is RLE-coding function. Based on the resulting code size $\langle f_{RLE}(B(r))\rangle$ (in bits), the partial compression ratios are calculated using the expression (3).

$$CR_{RLE}(r) = YX / \langle f_{RLE}(B(r))\rangle \tag{3}$$

at $r = \overline{0,R-1}$, where $\langle\ \rangle$ – represents the code size calculation operator.

TABLE I.
AVERAGE COMPRESSION RATIOS OF IMAGE BIT PLANES FOR THE RLE CODER

Bit planes	Partial and full compression ratios of bit planes of images				
	Grayscale satellite	Grayscale portrait	Grayscale medical	Landscape thermal	Differences of spectral channels
7 (15)	1.74466	1.56655	10.47579	1.17699	18318.4105 (1.4104)
6 (14)	1.12429	0.86344	3.50286	0.5182	18318.8455(50909.6075)
5 (13)	0.63831	0.6439	2.12782	0.34866	1157.6183(50909.6075)
4 (12)	0.42969	0.43127	1.10178	0.36688	1.1011 (50909.6075)
3 (11)	0.39203	0.40328	0.74446	0.33853	0.2947 (50909.6075)
2 (10)	0.40096	0.48656	0.50431	0.33297	0.2553 (50909.6075)
1 (9)	0.39986	0.50185	0.38566	0.36361	0.2450(45954.3425)
0 (8)	0.40006	0.44505	0.33411	0.38925	0.2494(36585.6001)
All	0.51390	0.52599	0.73092	0.40438	0.81049

TABLE II.
AVERAGE COMPRESSION RATIOS OF IMAGE BIT PLANES FOR THE ARITHMETIC CODER

Bit planes (high/low)	Partial (full) compression ratios high/low of bit planes of images			
	Grayscale satellite	Grayscale portrait	Grayscale medical	Landscape thermal
7/6–0	25.7676/1.0804 (1.2272)	13.0135/1.2382 (1.3941)	13.0135/1.6706 (1.8720)	27.4541/1.1168 (1.2689)
7–6/5–0	3.5595/1.0246 (1.2150)	2.2076/1.1635 (1.2982)	6.39613/1.5153 (1.8473)	2.8637/1.0581 (1.2550)
7–5/4–0	3.0243/1.0015 (1.3113)	1.9414/1.1058 (1.2886)	3.9399/1.3923 (1.7935)	2.2112/1.0244 (1.2816)
7–4/3–0	2.2277/0.9912 (1.3543)	1.7919/1.0650 (1.3209)	3.2933/1.2982 (1.8250)	1.9459/1.0045 (1.3239)
7–3/2–0	1.8680/0.9870 (1.3905)	1.6408/1.0244 (1.3295)	2.8619/1.2243 (1.8878)	1.7454/0.9925 (1.3578)
7–2/1–0	1.6625/0.9806 (1.4111)	1.5466/1.0208 (1.3577)	2.5539/1.1666 (1.9586)	1.5976/0.9827 (1.3810)
7–1/0	1.5246/0.9621 (1.4186)	1.4963/0.9358 (1.3821)	2.3217/1.0958 (2.0332)	1.4915/0.9649 (1.3958)

Encoding test images in their entirety (without splitting into bit planes) using the RLE coder does not result in compression ($\langle f_{RLE}(I(R))\rangle \geq RYX$).

The arithmetic coder is applied separately for higher ($f_{AC}(i_C(r_{HL}, r_{HH}, y, x))$) and lower ($f_{AC}(i_C(r_{LL}, r_{LH}, y, x))$) bit planes ($r_{HH} > r_{HL}, r_{LH} = r_{HL} - 1, r_{LH} > r_{LL}, r_{LL} \geq 0$), where f_{AC} is the function of arithmetic coding. Partial compression ratios are calculated using expressions (4) and (5).

$$CR_{AC}(r_{HL}, r_{HH}) = (r_{HH} - r_{HL} + 1)\,YX / \langle f_{AC}(I_C(r_{HL}, r_{HH}))\rangle \quad (4)$$

$$CR_{AC}(r_{LL}, r_{LH}) = (r_{LH} - r_{LL} + 1)\,YX / \langle f_{AC}(I_C(r_{LL}, r_{LH}))\rangle \quad (5)$$

The bit plane 15 of the differences of the HSI spectral channels contains the codes of the signs of the values of the differences: 0 – plus, 1 – minus and is encoded separately ($f_{AC}(B(15))$). Tables (I, II, and III) also show the full compression ratios $CR_{RLE}(R)$ and $CR_{AC}(R)$ of all bit-planes of the images, taking into account the volume of codes of individual bit-planes and their combinations, which are calculated using expressions (6) and (7).

$$CR_{RLE}(R) = \frac{RYX}{\sum_{r=0}^{R-1} \langle f_{RLE}(B(r))\rangle} \quad (6)$$

$$CR_{AC}(R) = \frac{RYX}{\langle f_{AC}(I_C(r_{HL}, r_{HH}))\rangle + \langle f_{AC}(I_C(r_{LL}, r_{LH}))\rangle} \quad (7)$$

Table I shows that the RLE coder allows compressing the two highest ($r = 7, 6$) medical bit-planes and one high ($r = 7$) bit-plane of portrait 8-bit grayscale images, as well as 9–11 high-order bit planes, starting from 14-th, of the differences of the spectral channels of HSI. For the remaining bit planes will not be used in compression. Moreover, even in the case of compression, the RLE coder is inferior in efficiency to the arithmetic coder on all types of images ($CR_{RLE}(r) > 1, CR_{RLE}(r) < CR_{AC}(r_{HL}, r_{HH})$, $CR_{RLE}(r) < CR_{AC}(r_{LL}, r_{LH})$), except for the differences in the HSI channels, which is associated with a high probability of zeros in their higher bit planes.

The use of an arithmetic coder for the lower bit-plane of 8-bit grayscale images ($\langle f_{AC}(I_C(0,0))\rangle > YX \Rightarrow CR_{AC}(0,0) < 1$) and 2 lower bit planes of 16-bit differences of the HSI channels ($\langle f_{AC}(I_C(0,1))\rangle > 2YX \Rightarrow CR_{AC}(0,1) < 1$), is usually

TABLE III.
AVERAGE COMPRESSION RATIOS OF BIT PLANES FOR DIFFERENCES IN THE HSI CHANNELS FOR THE ARITHMETIC CODER

Bit planes (high/low)	Partial (full) compression ratios high/low of bit planes of images	Bit planes (high/low)	Partial (full) compression ratios high/low of bit planes of images
15/14–0	0.5706/2.4806 (2.0414)	14–7/6–0	119.2902/1.1660 (2.6355)
14/13–0	15.6852/2.3152 (2.6180)	14–6/5–0	92.6252/1.0025 (2.6136)
14–13/12–0	31.3705/2.1498 (2.6180)	14–5/4–0	94.0904/0.8537 (2.6491)
14–12/11–0	47.0557/1.9844 (2.6180)	14–4/3–0	93.4257/0.7415 (2.7321)
14–11/10–0	62.7409/1.8191 (2.6180)	14–3/2–0	22.6167/0.6888 (2.9558)
14–10/9–0	78.4262/1.6537 (2.6180)	14–2/1–0	6.5078/0.6497 (3.0008)
14–9/8–0	94.1114/1.4883 (2.6180)	14–1/0	3.9643/0.6073 (3.0477)
14–8/7–0	109.7933/1.3235 (2.6191)		

not effective. In other cases, the arithmetic coder provides compression of individual bit planes and their combinations. Moreover, when coding the higher bit planes of differences in the HSI channels, the arithmetic coder shows the worst results in comparison with the RLE coder.

When coding test images in their entirety (without separation into bit-planes) using the arithmetic $(f_{AC}(I(R)))$ and RLE $(f_{RLE}(I(R)))$ coders, the following average compression ratios were obtained: satellite images – CR_{AC} =1.22 and CR_{RLE} = 0.95 times; portrait images – CR_{AC} =1.35 and CR_{RLE} =1.04 times; medical images – CR_{AC} =1.86 and CR_{RLE} =1.62 times; landscape thermal images – CR_{AC} =2.13 and CR_{RLE} =1.69 times; differences of HSI channels – CR_{AC} =2.29 and CR_{RLE} =1.02 times. The comparison of these results with the data given in Tables (I, II, and III), shows that separate coding of bit planes $(f_{RLE}(B(r))$ at $r=\overline{0,R-1}$ and $f_{AC}(I_C(r_{HL},r_{HH})), f_{AC}(I_C(r_{LL},r_{LH}))$ at $r_{HH}=R-1, r_{HH}>r_{HL}, r_{LH}=r_{HL}-1, r_{LH}>r_{LL}, r_{LL}=0)$ allows to increase the compression ratio of images compared to their direct coding $(f_{RLE}(I(R))$ and $f_{AC}(I(R)))$.

III. COMBINED EFFECTIVE CODING OF IMAGE BIT PLANES

To increase the lossless image compression ratio, the combined effective coding is used. Its essence consists in using to compress the highest image bit planes or their combinations, several coders of various types $(f_{RLE}(B(r))$ and $f_{AC}(I_C(r_{HL},r_{HH})))$, better taking into account the distribution of their values, and directly incorporate in the coding result of the lower bit planes $(f_{NC}(B(r))$ at $r\geq 0$ or $f_{NC}(I_C(0,r_{LH}))$ at $r_{LH}\geq 0)$, the coding of which is not effective $(\langle f_{RLE}(B(r))\rangle \geq YX$ at $r\geq 0$ or $\langle f_{AC}(I_C(0,r_{LH}))\rangle \geq (r_{LH}+1)YX$ at $r_{LH}\geq 0)$, as shown in Fig. 3, where f_{NC} – is the direct transfer function of the lower bit planes without coding.

Tables (I, II, and III) show that combined coding is effective for compressing the differences of HSI channels.

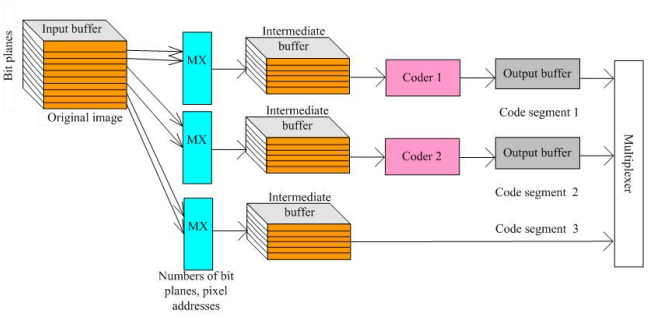

Fig. 3. Combined effective coding of image bit planes scheme

HSI $P=\{P(i)\}_{(i=\overline{0,N_C-1})}$ is a collection N_C of spectral channels $P(i)=\|P(y,x,i)\|_{(y=\overline{0,Y-1},x=\overline{0,X-1})}$ of size $Y\times X$ pixels and bit depth D_B. Each spectral channel corresponds to a specific part of the spectrum.

To estimate the pixel correlation of the i–th $P(i)$ and j–th $P(j)$ HSI channels, the values of mean error $ME_P(i,j)$ are used, which is calculated using (8).

$$ME_P(i,j)=\sum_{y=0}^{Y-1}\sum_{x=0}^{X-1}|p(y,x,i)-p(y,x,j)|/(YX) \quad (8)$$

where $|\ |$ – is modulo operation.

Fig. 4(a) shows the dependence of $ME_P(i,j)$ on the spectral channel number at $i=24$ and $j=\overline{0,N_C-1}$, $N_C=68$.

To estimate the bitwise correlation of the b-th bit planes of the i–th $P(i)$ and j–th $P(j)$ channels of hyperspectral images HSI, the values of mean error $ME_B(b,i,j)$ are used, which is calculated using (9).

$$ME_B(b,i,j)=\frac{\sum_{y=0}^{Y-1}\sum_{x=0}^{X-1}(p(y,x,b,i)\oplus p(y,x,b,j))}{YX} \quad (9)$$

where $\oplus$ – operation ≪Exclusive OR≫.

For example, in Fig. 4(b, c, d) are shown the dependences of $ME_B(b,i,j)$ on the spectral channel number at $i = 24$, $b = \{12,5,0\}$ and $j = \overline{0,N_C-1}$, $N_C = 68$.

Fig. 3 shows that, HSI bit planes have different correlation properties. Higher planes determine the general form of the error distribution function, while lower planes practically do not correlate and slightly affect the general form of the error distribution function.

Table IV shows the most effective combinations of arithmetic and RLE coders for the bit planes of the four differences of adjacent channels of the test HSI taken from the Aviris database [24], and the compression ratios CR_C, corresponding to these combinations.

The compression ratio for combined effective coding is calculated using (10).

$$CR_C = \frac{RYX}{S_1+S_2+S_3} \tag{10}$$

where S_1, S_2, S_3 are calculated by using the expressions (11), (12), and (13) respectively.

$$S_1 = \sum_{m=1}^{M} \langle f_{RLE}(B(r(m))) \rangle \tag{11}$$

$$S_2 = \sum_{n=1}^{N} \langle f_{AC}(I_C(r_L(n), r_H(n))) \rangle \tag{12}$$

$$S_3 = \sum_{p=0}^{P-1} \langle f_{NC}(B(p)) \rangle \tag{13}$$

at $R = M+N+P$, $r_H(n) > r_L(n)$, $M \geq 0$, $N \geq 0$, $P \geq 0$, where M – is the number of bit planes encoded using the RLE coder; N – is the number of bit planes encoded using the arithmetic coder; P – is the number of bit planes, directly transferred to the resulting code.

Based on the Table IV, the following rule of combined coding of differences of neighboring HSI channels is proposed, which determines the formation of the resulting code C_C: it is necessary to use the arithmetic coder for the highest sign plane and bit planes 8–2, the RLE coder – for bit planes 14–9, transfer without coding – for bit planes 1–0, which is determined by (14).

$$C_C \leftarrow f_{AC}(B(15)) \oplus f_{RLE}(B(14)) \oplus \cdots \oplus f_{RLE}(B(9)) \oplus f_{AC}(I_C(2,8)) \oplus f_{NC}(I_C(0,1)) \tag{14}$$

it provides the code size $\langle C_C \rangle$, equal to (15).

$$\langle C_C \rangle = \langle f_{AC}(B(15)) \rangle + \sum_{r=9}^{14} \langle f_{RLE}(B(r)) \rangle + \langle f_{AC}(I_C(2,8)) \rangle + \langle f_{NC}(I_C(0,1)) \rangle \tag{15}$$

and compression ratio $\overline{CR_C}$, equal to (16).

$$\overline{CR_C} = \frac{16YX}{\langle C_C \rangle} \tag{16}$$

where $\oplus$ – is the concatenation operator, which forms the resulting code from the fragments, corresponding to bit planes and their combinations.

From Table IV, it follows that combined coding allows to increase the compression ratio of the differences of neighboring HSI channels by an average of $CR_C/CR_{AC} = 1.4$ and $CR_C/CR_{RLE} = 3.1$ times compared to arithmetic and RLE-coding respectively.

The proposed rule allows to synthesize the structure of HSI coder as shown in Fig. 5. It consists of a combined coder of differences of HSI channels and a HSI reference channel coder. The combination of arithmetic and RLE coders as a part of the coder of the differences of HSI channels differs from the effective combinations considered in Table IV, which leads to a decrease in compression ratio, but does not require the use of additional switching and control units in codecs. The gain in the compression ratio of the differences of the neighboring HSI channels is on average $\overline{CR_C}/CR_{AC} = 1.2$ and $\overline{CR_C}/CR_{RLE} = 2.6$ times compared to arithmetic and RLE-coding, respectively. To encode the HSI reference channel, the arithmetic coder is used, to which 12 high-order bit planes of the reference channel are fed, and 4 lower-order bit planes are directly transferred to the resulting code. This structure follows from an analysis of the effectiveness of separate coding of bit planes of HSI channels, which shows that, as a rule, from 2 to 6 lower bit planes are not compressed using the arithmetic coder.

In Tables V, VI are shown the compression ratios of the higher and lower bit planes for the 24th spectral channel of 16-bit HSI-1, as shown in Fig. 6, and HSI-2 with dimensions of 2048×614 and 1024×614 pixels, respectively.

Tables V and VI, show that the coding of the lower bit planes of the spectral channels in some cases is not effective and the compression ratio of the HSI can be increased by using the lower bit planes without coding.

The arithmetic coding (AC) blocks are considered the most computationally complex elements of the HSI coder. They are operating at frequencies $YXC_{AC}f$ and $YXC_{AC}f/(N-1)$ in the part of coders of the differences of spectral channels and reference channel of HSI, respectively, where N – is the

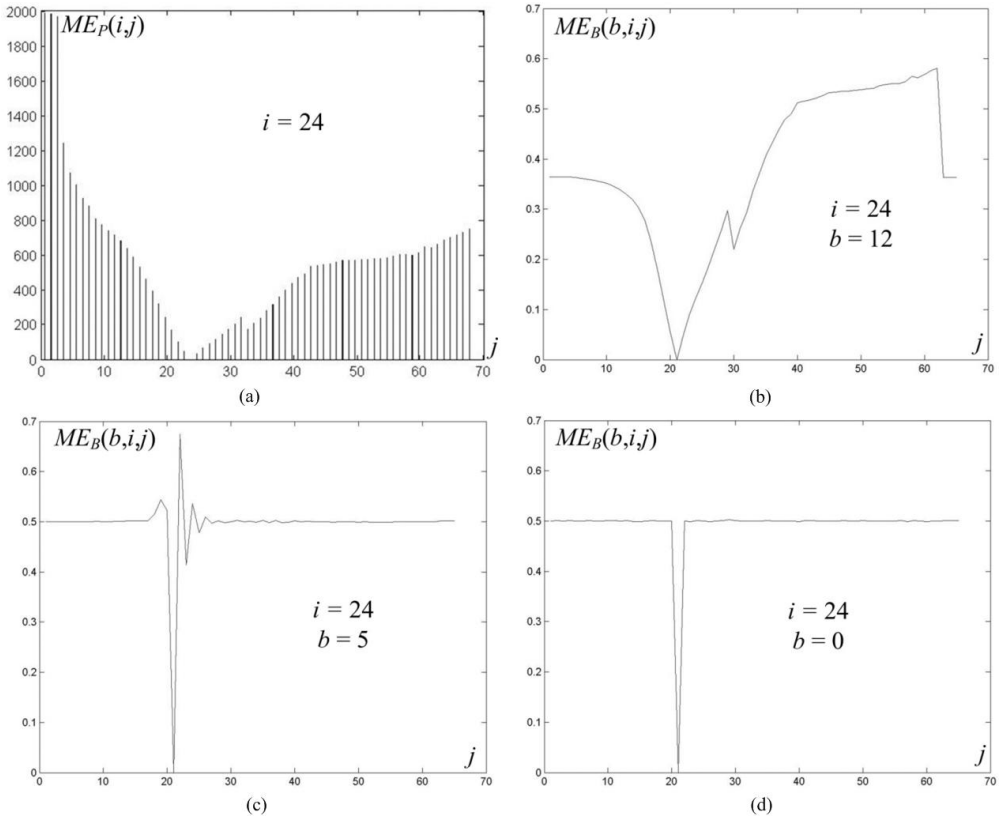

Fig. 4. Dependences of the mean error on the spectral channel number: (a) for pixel inter-channel correlation; (b) for bitwise inter-channel correlation (12th bit plane); (c) for bitwise inter-channel correlation (5th bit plane); (d) for bitwise inter-channel correlation (0th bit plane)

number of spectral channels; $C_{AC} > 1$ – is a coefficient taking into account the computational (time) complexity of the arithmetic coder compared to RLE (operate at frequency YXf); f – is clock frequency $f = Nf_I$; f_I – is HSI formation frequency. It is found, experimentally, that $C_{AC} \approx 11$.

The structure of HSI coder also includes spectral channel multiplexers, operating at a frequency f at the control inputs and at a frequency $16YXf$ at the data inputs; a multiplexer of codes of bit planes of differences of spectral channels, operating at a frequency $10f$; a multiplexer of codes of bit planes of reference channel, operating at a frequency $5f/(N-1)$; a multiplexer of reference codes and differences of HSI channels, operating at a frequency $f/(N-1)$. In a sequential implementation, the computational complexity of the combined coder is about $2YXC_{AC}f + 6YXf$ at a large number of spectral channels, which is about 2.5 and 28 times more than arithmetic and RLE-coding, respectively.

Figure 7 shows the structure of combined HSI decoder.

IV. Conclusion

In this paper, a combined codec structure for compressing bit planes of images without loss in the spatial domain based on arithmetic and RLE coders is proposed. The efficiency of combined coding for compressing channel differences of hyperspectral images is established. The choice of optimal combinations of bit planes for arithmetic and RLE coding allows to increase the compression ratio of the differences of neighboring HSI channels by an average of 1.4 and 3.1 times compared to arithmetic and RLE coding, respectively. A rule has been developed for combined coding of differences of adjacent channels of hyperspectral images, using arithmetic coding for the upper sign plane and bit planes 8–2, RLE coding for bit planes 14–9, and transfer without coding for bit planes 1–0, which made it possible to increase the compression ratio of the differences of neighboring channels of hyperspectral images on average 1.2 and 2.6 times compared to arithmetic and RLE coding, respectively, with an increase in computational complexity of 2.5 and 28 times. Based on this rule, the coder structure of hyperspectral images

TABLE IV.
THE MOST EFFECTIVE COMBINATIONS OF ARITHMETIC AND RLE CODERS AND COMPRESSION RATIOS

Bit planes	Combinations of arithmetic and RLE coders for differences of HSI channels							
	Difference 1		Difference 2		Difference 3		Difference 4	
15|7	RLE	RLE	AC	RLE	AC	AC	RLE	AC
14|6	RLE	RLE	RLE	RLE	RLE		RLE	
13|5	RLE	RLE	RLE	RLE	RLE		RLE	
12|4	RLE	AC	RLE	AC	RLE		RLE	NC
11|3	RLE		RLE		RLE		RLE	NC
10|2	RLE	NC	RLE		RLE	NC	RLE	NC
9|1	RLE	NC	RLE	NC	RLE	NC	RLE	NC
8|0	RLE	NC	RLE	NC	RLE	NC		NC
CR_C	3.72917		3.16748		3.15484		2.80657	
CR_{AC}	2.53492		2.29310		2.16147		2.18485	
CR_{RLE}	1.02866		0.97902		1.04260		1.03313	
$\overline{CR_C}$	2.46175		3.16773		3.07913		1.93187	

is developed.

CONFLICT OF INTEREST

The authors have no conflict of relevant interest to this article.

REFERENCES

[1] H. Irmak, G. B. Akar, and S. E. Y. uksel, "Image fusion for hyperspectral image super-resolution," in *2018 9th Workshop on Hyperspectral Image and Signal Processing: Evolution in Remote Sensing (WHISPERS)*, pp. 1–5, 2018.

[2] O. Ozdil, A. Gunes, Y. E. Esin, S. Ozturk, and B. Demirel, "4-stage target detection approach in hyperspectral images," in *2018 9th Workshop on Hyperspectral Image and Signal Processing: Evolution in Remote Sensing (WHISPERS)*, pp. 1–5, 2018.

[3] M. Zhao, C. Yu, M. Song, and C.-I. Chang, "A semantic feature extraction method for hyperspectral image classification based on hashing learning," in *2018 9th Workshop on Hyperspectral Image and Signal Processing: Evolution in Remote Sensing (WHISPERS)*, pp. 1–5, 2018.

[4] F. Arias, H. Sierra, and E. Arzuaga, "A framework for an artificial neural network enabled single pixel hyperspectral imager," in *2019 10th Workshop on Hyperspectral Imaging and Signal Processing: Evolution in Remote Sensing (WHISPERS)*, pp. 1–5, 2019.

[5] O. J. M. Al-Furaiji, "Resolution enhancement of images pair based on block cross interpolation," *Periodicals of Engineering and Natural Sciences*, vol. 8, no. 2, pp. 1067–1074, 2020.

[6] O. J. M. Al-Furaiji, V. V. Rabtsevich, V. Y. Tsviatkou, T. A. Kuznetsova, and S. A. Chizhik, "Segmentation of afm-images based on wave region growing of local maxima," *Engineering Letters*, vol. 28, no. 3, pp. 681–698, 2020.

[7] S. Shirani, "Data compression: The complete reference (by d. salomon; 2007)[book review]," *IEEE Signal Processing Magazine*, vol. 25, no. 2, pp. 147–149, 2008.

[8] V. Bhaskaran and K. Konstantinides, *Image and video compression standards: algorithms and architectures*. Springer Science & Business Media, 1997.

[9] R. C. Gonzalez, *Digital image processing*. Pearson education india, 2009.

[10] J. Ziv and A. Lempel, "A universal algorithm for sequential data compression," *IEEE Transactions on information theory*, vol. 23, no. 3, pp. 337–343, 1977.

[11] D. S. Taubman, M. W. Marcellin, and M. Rabbani, "Jpeg2000: Image compression fundamentals, standards and practice," *Journal of Electronic Imaging*, vol. 11, no. 2, pp. 286–287, 2002.

[12] J. M. Shapiro, "Embedded image coding using zerotrees of wavelet coefficients," *IEEE Transactions on signal processing*, vol. 41, no. 12, pp. 3445–3462, 1993.

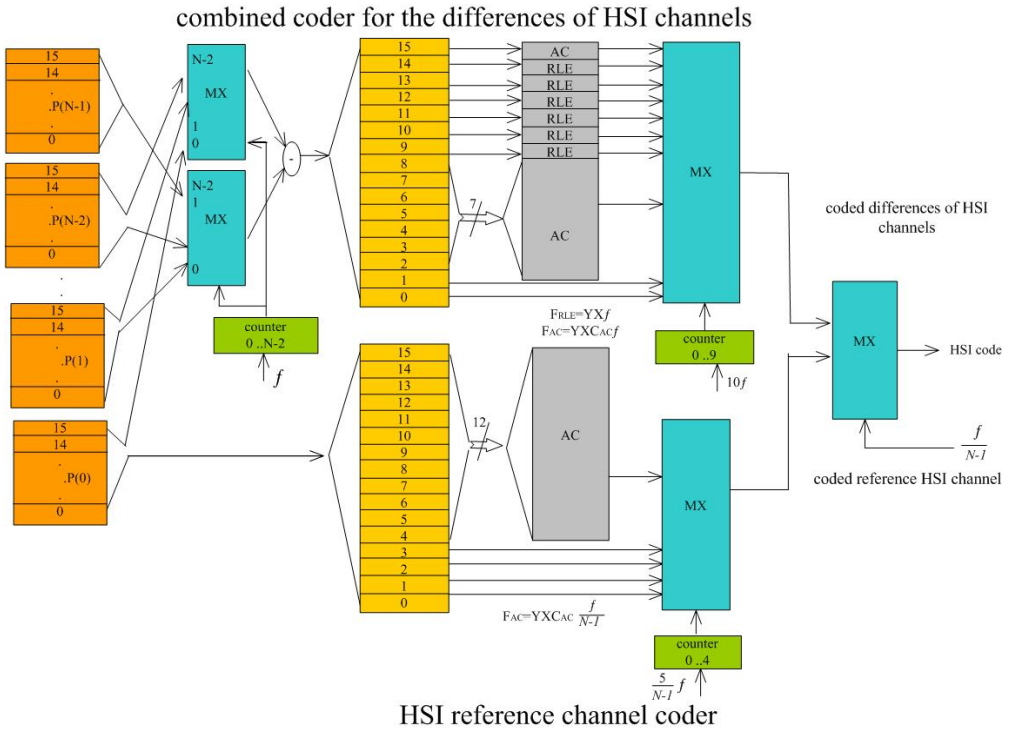

Fig. 5. Structure of combined coder for hyperspectral images

Fig. 6. 24th HSI-1 spectral channels

[13] Y. Xu and J. Zhang, "Invertible resampling-based layered image compression," in *2021 Data Compression Conference (DCC)*, pp. 380–380, IEEE, 2021.

[14] E. Abderraouf, M. R. Lahcene, M. S. Bendelhoum, S. A. Zegnoun, A. A. Tadjeddine, and F. Menezla, "Transmission performance in compressed medical images using turbo code," *Indonesian Journal of Electrical Engineering and Computer Science*, vol. 27, no. 1, pp. 318–327, 2022.

[15] D. Sivaraman, J. Jebanazer, and B. Balasubramanian, "Discriminative analysis of wavelets for efficient medical image compression," *Indonesian Journal of Electrical Engineering and Computer Science*, vol. 30, no. 1, pp. 510–517, 2023.

[16] Z. Abood, S. Abood, and T. Ismaeel, "Comparison hybrid techniques-based mixed transform using compression and quality metrics," *Indonesian Journal of Electrical Engineering and Computer Science*, vol. 30, no. 2, pp. 807–816, 2023.

[17] A. Said and W. Pearlman, "A new, fast, and efficient image codec based on set partitioning in hierarchical trees," *IEEE Transactions on Circuits and Systems for Video Technology*, vol. 6, no. 3, pp. 243–250, 1996.

[18] A. Islam and W. Pearlman, "Set partitioned sub-block coding (speck)," *ISO/IEC/JTC1/SC29, WG1*, no. 873, pp. 312–326, 1998.

[19] H. K. Al-Bahadily, A. A. J. Altaay, V. Tsviatkou, and V. Konopelko, "New modified RLE algorithms to compress grayscale images with lossy and lossless compression," *International Journal of Advanced Computer Science and Applications*, vol. 7, no. 7, pp. 250–255, 2016.

[20] N. Abramson, *Information Theory and Coding*. McGraw Hill; First Edition, 1963.

[21] M. K. Abdmouleh, A. Masmoudi, and M. S. Bouhlel, "A new method which combines arithmetic coding with RLE for lossless image compression," *Journal of Software Engineering and Applications*, no. 5, 2012.

TABLE V.
COMPRESSION RATIOS OF ONE HSI-1 CHANNEL (2048×614 PIXELS)
WITH BITWISE CHANNEL-BY-CHANNEL ENTROPY CODING

Bit planes of the 24th spectral channel	Original size of bit planes, bytes	Bit planes size after coding, bytes	Compression ratio
15/14–0	157184 / 2357760	2613/1883521	60.15/1.25
15–14/13–0	314368/ 2200576	2613/1883521	120.31/1.17
15–13/12–0	471552 / 2043392	2613/1883521	180.46/1.08
15–12 / 11–0	628736 / 1886208	2613/1883375	240.62/1.00
15–11 / 10–0	785920 / 1729024	4132/1874820	190.20/0.92
15–10 / 9–0	943104 / 1571840	95456/1829138	9.88/0.86
15–9 / 8–0	1100288 / 1414656	104891/1750699	10.49/0.81
15–8 / 7–0	1257472 / 1257472	159139/1594979	7.90/0.79
15–7 / 6–0	1414656 / 1100288	278260/1369337	5.08/0.80
15–6 / 5–0	1571840 / 943104	443957/1190758	3.54/0.79
15–5 / 4–0	1729024 / 785920	649261/1010438	2.66/0.78
15–4 / 3–0	1886208 / 628736	878460/807483	2.15/0.78
15–3 / 2–0	2043392 / 471552	1112691/613273	1.84/0.77
15–2 / 1–0	2200576/314368	1349571/412672	1.63/0.76
15–1 / 0	2357760/157184	1561168/217577	1.51/0.72

[22] S. Golomb, "Run-length encodings (corresp.)," *IEEE transactions on information theory*, vol. 12, no. 3, pp. 399–401, 1966.

[23] F. Rubin, "Arithmetic stream coding using fixed precision registers," *IEEE Transactions on Information Theory*, vol. 25, no. 6, pp. 672–675, 1979.

[24] [NULL], "AVIRIS - Airborne Visible / Infrared Imaging Spectrometer - Data — aviris.jpl.nasa.gov." https://aviris.jpl.nasa.gov/data/index.html. [Accessed 16-Jul-2023].

TABLE VI.
COMPRESSION RATIOS OF ONE HSI-2 CHANNEL (1024×614 PIXELS)
WITH BITWISE CHANNEL-BY-CHANNEL ENTROPY CODING

Bit planes of the 24th spectral channel	Original size of bit planes, bytes	Bit planes size after coding, bytes	Compression ratio
15/14–0	78592/1178880	1398/940935	56.22/1.25
15–14/13–0	157184/1100288	1398/940935	112.43/1.17
15–13/12–0	235776/1021696	1398/940902	168.65/1.09
15–12 / 11–0	314368/943104	1617/939452	194.41/1.00
15–11 / 10–0	392960/864512	6621/929097	59.35/0.93
15–10 / 9–0	471552/785920	61584/898299	7.66/0.87
15–9 / 8–0	550144/707328	80538/866182	6.83/0.82
15–8 / 7–0	628736/628736	127599/789177	4.93/0.80
15–7 / 6–0	707328/550144	201035/690999	3.52/0.80
15–6 / 5–0	785920/471552	291767/594516	2.69/0.79
15–5 / 4–0	864512/392960	397326/503015	2.18/0.78
15–4 / 3–0	943104/314368	511096/401267	1.85/0.78
15–3 / 2–0	1021696/235776	626245/307106	1.63/0.77
15–2 / 1–0	1100288/157184	737514/206867	1.49/0.76
15–1 / 0	1178880/78592	828813/109069	1.42/0.72

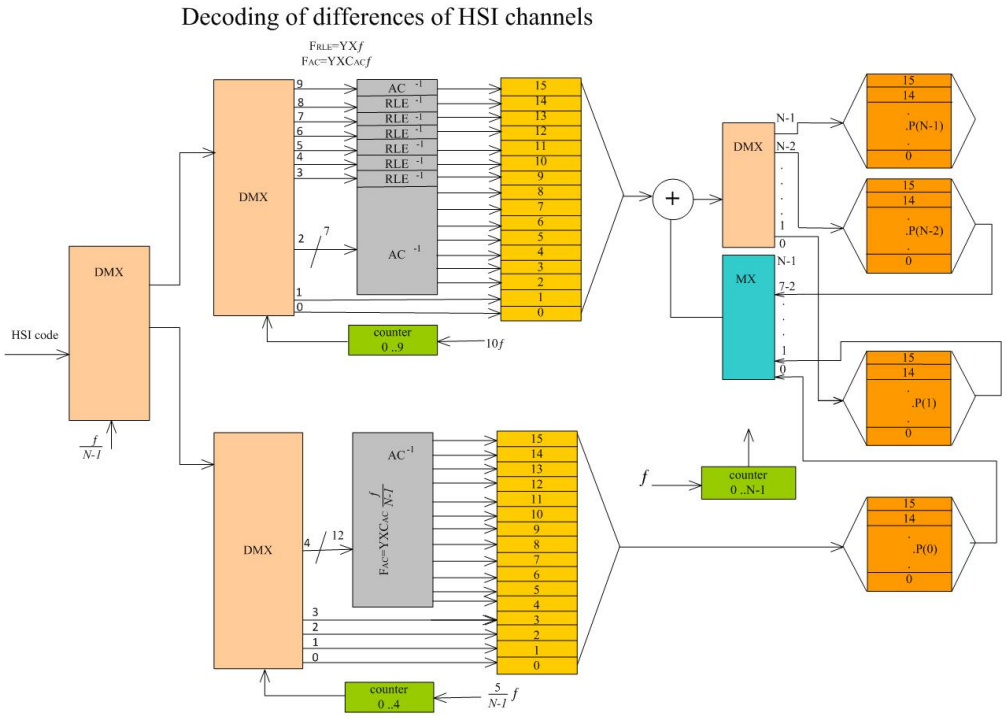

Fig. 7. Structure of combined decoder for hyperspectral images